Linearization Method for Large-scale Hydro-thermal Security-Constrained Unit Commitment

Ming Qu, *Student Member, IEEE,* Tao Ding, *Senior Member, IEEE,* Chenggang Mu, *Student Member, IEEE,* Xiaosheng Zhang, Kai Pan, *Member, IEEE,* Mohammad Shahidehpour, *Fellow, IEEE*

***Abstract*—Security-constrained unit commitment (SCUC) is one of the most fundamental optimization problems in power systems. The objective of SCUC is to minimize the operating cost while respecting both system-wide and generator-specific constraints. It leads to a large-scale and mixed-integer programming (MIP) model with a large number of binary decision variables which is difficult to solve. This paper, based on the convex hull theory of single-unit, proposes a linearization method for the hydro-thermal SCUC problem with decoupled thermal units and variable-head hydro units. Then, the strategy of embedding two types of convex hulls in a multi-unit commitment and the heuristic method of constructing a feasible solution are designed, by which the multi-UC is approximated from large-scale mixed-integer programming to linear programming that can be solved in polynomial time. Finally, we theoretically prove that the optimal solution of the proposed LP model is always better than that of the Lagrangian Relaxation model. Numerical experiments on several large-scale test systems demonstrate the effectiveness and efficiency of the proposed method.**

***Note to Practitioners*—This paper proposes a linear programming model for the SCUC problem by lifting up to a higher-dimensional space. It realizes an important innovation in reducing the computational complexity of SCUC from the perspective of linearization. The proposed method can be well applied to large-scale long-term unit commitment problems. To better use this method, the following two properties should be highlighted: i) the error of the proposed method is less than the Lagrangian relaxation method and decreases with the increasing system scales; ii) the computational efficiency of the proposed method is 10-100 times faster than that of the MIP model. We have tested many practical power systems and find that the error of the proposed LP model is usually very small compared with the precise MIP while the computational performance is significantly improved. In some practical cases, the decision makers usually do not want to find the precise optimal solution while only an approximation under a fast speed, because the boundary condition is imprecise. The proposed method is useful. Besides, for the cases that need the precise optimal solution, the proposed method can provide a high-quality initial solution for the MIP model to accelerate the convergence.**

***Index Terms*—Security-Constrained Unit Commitment (SCUC), Convex Hull, Hydro-thermal Units, Lagrangian Relaxation**

NOMENCLATURE

Indices and Sets

t	Index of dispatching periods
g	Index of units
l	Index of transmission lines
b	Index of buses
G/H	Set of thermal/hydro units
L	Set of transmission lines
Bus	Set of buses
$\mathbb{R}$	Set of real numbers
$\mathbb{B}$	Set of binary numbers
$\mathbb{Z}$	Set of integer numbers
$\mathcal{G}$	Set of all the possible continuous "on" intervals
$\mathcal{Q}$	Set of all the possible optimal generation amounts under different conditions
$\mathcal{E}$	Set of all the possible optimal states which can be described as quaternions including optimal generation amounts and on/off status
$\mathcal{E}_0$	A dummy source state as the initial status of the generator before period 1
$\Theta_{\mathcal{G}}^{\mathrm{LP}}$	Feasible region of the $\mathcal{G}$ -convex hull
$\Theta_{\mathcal{E}}^{\mathrm{LP}}$	Feasible region of the $\mathcal{E}$ -convex hull
Θ^{MILP}	Feasible region of the MILP model
$\Gamma_{\Rightarrow i}$	All the immediate successors of state e_i ($e_i \in \mathcal{E}$)
$\Gamma_{i\Rightarrow}$	All the immediate predecessors of status e_i ($e_i \in \mathcal{E}$)
$\Psi^{p,\mathrm{LP}}$	Feasible region of the LP model for single hydro unit
$\Psi^{\mathrm{hydro,LP}}$	Feasible region of the LP model of the hydro generator
$\Psi^{\mathrm{pump,LP}}$	Feasible region of the LP model of the pump
$\Psi^{\mathrm{hydro,MILP}}$/ $\Psi^{\mathrm{pump,MILP}}$	Feasible region of the MILP model for the normal hydro units/pumping storage units
Φ_0	Set of units always in off-status
Φ_1	Set of units with the binary optimal solution
Φ_*	Set of units with the fractional optimal solution
E_{1t}	Set of units in on-status and without ramp rate constraints at time t
E_{2t}	Set of units in on-status and the time period t is the first/last period of the entire "on" interval
E_{3t}	Set of units with ramp rate constraints at time t
$\lvert * \rvert$	The cardinality of Set *

Parameters and Functions

T	Number of scheduling periods (h)
$C^{\mathrm{start}}/C^{\mathrm{shut}}$	Start-up/shut-down cost of generators ($)
$T^{\mathrm{on}}/T^{\mathrm{off}}$	Minimum-up/-down time limits (h)
$P^{\max}/P^{\min}$	Maximum/minimum generation outputs of a generator (MW)
R^0	Start-up/shut-down ramp rate limits (MW/h)
R^1	Ramp-up/-down rate (MW/h)
e_i / e_j	i/j-th element in $\mathcal{E}$ representing the optimal state
$\eta^{\mathrm{w\text{-}e}}$	Conversion coefficient of water-to-electricity
$\eta^{\mathrm{e\text{-}w}}$	Conversion coefficient of electricity-to-water
$V^{\mathrm{up,max}}/$ $V^{\mathrm{up,min}}$	Upper and lower bounds of the upstream reservoir capacity (m)
$V^{\mathrm{dn,max}}/$ $V^{\mathrm{dn,min}}$	Upper and lower bounds of the downstream reservoir capacity (m)
U_t^{up} / U_t^{dn}	Natural inflows of upstream/downstream reservoir at time t (m^3)
$D_{b,t}$	Load of bus b at time t (MW)
r_t	Reserve capacity requirement at time t (MW)
H^{PTDF}	Power transmission distribution factor matrix
$F_l^{\max}$	Transmission limit of the l-th transmission line (MW)
$O(*)$	Time complexity of an algorithm
$\psi_1(\mathrm{V})$	Nonlinear head-volume function of upstream reservoir

$\psi_2(*)$	Nonlinear head-volume function of downstream reservoir

Variables

$P_t\,(P_{g,t})$	Generation amount (of the g-th unit) at time t
$x_t\,(x_{g,t})$	Binary variable to indicate whether a generator is on at time t ($x_t\,(x_{g,t})$=1) or not ($x_t\,(x_{g,t})$=0)
$u_t\,(u_{g,t})$	Binary variable to indicate whether a generator starts up at time t ($u_t\,(u_{g,t})$=1) or not ($u_t\,(u_{g,t})$=0)
$v_t\,(v_{g,t})$	Binary variable to indicate whether a pump starts up at time t ($u_t\,(u_{g,t})$=1) or not ($u_t\,(u_{g,t})$=0)
$z_t(z_{g,t})$	Binary variable to indicate whether a pump storage station is pumping ($z_t(u_{g,t})$=1) or not ($z_t(u_{g,t})$ =0)
α_t	Binary variable to indicate whether a generator starts up for the first time at time t (α_t=1) not (α_t =0)
$\beta_{t,k}$	Binary variable to indicate whether a generator is on throughout the entire interval $[t,k]_{\mathbb{Z}}$ ($\beta_{t,k}$=1, i.e., starts up at time t and shuts down at time k+1) or not ($\beta_{t,k}$ =0)
$\gamma_{t,k}$	Binary variable to indicate whether a generator is off throughout the entire interval $[t+1,k-1]_{\mathbb{Z}}$ ($\gamma_{t,k}$ =1 i.e., shuts down at time t+1 and starts up again at time k+1) or not ($\gamma_{t,k}$ =0)
χ_t	Binary variable to indicate whether a generator is off throughout the entire interval $[t+1,T]_{\mathbb{Z}}$ (χ_t =1, i.e., shuts down at time t+1 and stays offline to the end) or not (χ_t =0)
$\rho_{t,k}^{\tau}$	Generation amount at time τ if a generator is on throughout the entire interval $[t,k]_{\mathbb{Z}}$
λ_{ij}	Binary variable to indicate whether the optimal decision corresponds to a state changes from state e_i at time t-1 to state e_j at time t (λ_{ij}=1) or not (λ_{ij}=0)
W_t^{hydro}	Water consumption of power units at time t
W_t^{pump}	Pumping capacity of pumping units at time t
P_t^{hydro}	Power generation of power units at time t
P_t^{pump}	Power consumption of pumping units at t
V_t^{up} / V_t^{dn}	Reservoir volume of the upstream /downstream reservoir

I. Introduction

Security-constrained unit commitment (SCUC) is one of the most fundamental optimization problems in power systems. It is widely used for renewable energy consumption [1], power system operation [2], power market clearing [3], and power system resilience [4], among others. The objective of SCUC is to minimize the system operating cost while respecting both system-wide and generator-specific constraints. It leads to a large-scale and mixed-integer optimization problem with a large number of binary decision variables. How to solve such a difficult problem efficiently remains a critically important topic of research for decades.

Lagrangian relaxation (LR) and mixed-integer programming (MIP) [5] are two types of methods that are generally recognized and have been widely applied in engineering. The LR decomposes multi-unit SCUC (multi-UC) models into several single-unit UC (single-UC) models [6] by relaxing the coupling constraints (e.g., demand balance constraints). The duality gap of LR was set as the convergence criterion, and then the feasible suboptimal solution of the primal problem was constructed based on the dual solution of LR [7]. To apply the LR model to solve the long-term SCUC model, a hybrid subgradient and Dantzig-Wolfe decomposition method was established in [8] to manage Lagrangian multipliers. The LR model was widely used in the past decades due to its high computational efficiency [9]. However, a major drawback is that convergence is not guaranteed, particularly when the system constraints become more complex. With the development of more advanced MIP algorithms (e.g., branch-and-cut), the application of MIP to solve SCUC has received more attention [10]-[13]. A temporal decomposition strategy was proposed in [11] to reduce the computational time of SCUC by using the Nesterov momentum for gradient methods to coordinate sub-problems in a distributed way. The solution time was decreased by 94% over the IEEE 118-bus system. Ref. [12] applied the Benders decomposition algorithm to solve the tri-level SCUC model, considering transmission outages in the security criterion. Numerical results showed that the algorithm significantly reduced the computing memory requirement. Taking into account the dynamic constraints of hydro units, [13] presented the application of the MIP model in solving the stochastic hydrothermal SCUC. In the hydrothermal unit commitment problem, it's crucial to accurately model the nonlinear hydropower generation function. Thus, a three-dimensional interpolation technique was used in [14], while Ref [15] proposed an efficient linear approximation method based on the variable separation and piecewise linear technique. The results showed that the approximate error of the above method was very small. Furthermore, the detailed comparisons between LR-based and MIP-based methods were discussed in [16] in terms of modeling ability, feasibility and optimality, solution stability, computer resource consumption, hot-start capability, and application.

Due to continuously increasing demand, the number of units in power systems has increased dramatically. Few algorithms can fully balance the optimal solution quality and computational efficiency of SCUC. Although commercial solvers (e.g., GUROBI [17] and CPLEX [18]) and some acceleration algorithms (e.g., variable reduction [19] and redundant security constraints reduction [20]) can alleviate this situation, the NP-Hardness nature keeps the SCUC problem as a difficult one. In addition, the rapid development of renewable energy introduces uncertainty, which makes the unit commitment model more complex [21]. Stochastic optimization [22], robust optimization [23], and distributionally robust optimization [24],[39] are the most popular methods of addressing this problem. Therefore, solving large-scale SCUC quickly and efficiently remains an urgent problem.

To address such a challenge, there exist studies focusing on deriving algorithms to tighten or reformulate the SCUC model that can hopefully transform it from an MIP problem to a linear programming (LP) problem, by which the computational complexity can be reduced. To that end, the convex hull formulations of the SCUC model may be derived. The convex hull is the convex relaxation of nonconvex problems that can transform the mixed-integer linear programming (MILP) model into an LP model. The convex hull formulations or tighter (strong) valid inequalities are often used to strengthen the MILP formulation, improving the computational performance. However, those MILP formulations may still be difficult to

solve because of the many integer variables involved in the large-scale SCUC [25]. In addition, the convex hull formulations are also widely used to perform convex hull pricing [26],[37], which more accurately prices each asset in the power systems. Ref. [27] calculated the ranges of the remaining variables' values by fixing one of the variables. A set of feasible solutions was obtained after searching each variable, and the convex hull was generated with these feasible solutions. In [28], based on a feasible solution, the neighborhood search algorithm was used to relax the MIP problem, and then an iterative compression algorithm was proposed to tighten the constraints to obtain a tight formulation. A convex hull was established in [29] by the integration of three steps: "constraint-and-vertex conversion," "vertex elimination" and "parameterization". The above convex hulls were all obtained from the mathematical view of MIP by enumeration and relaxation. However, the physical characteristics of the SCUC were not considered in the above approaches, which may lead to two issues: (i) They could not handle models containing complex system and unit constraints; (ii) The speed of forming convex hulls is slow, especially for large-scale systems.

Different from the above methods, [30] proposed two types of convex hulls for thermal single-UC by studying all the possible "on" intervals and all the possible optimal generation amounts, respectively. These two convex hulls were theoretically proved to be equivalent to the original MILP model with a piecewise linear objective function. However, the models in [30] were designed for the single thermal unit, and could be applied to neither hydro single-UC nor multi-UC, both of which were critically important for current power system operations. We note that no studies have provided a systematic large-scale SCUC solution to solve the above two issues from the perspective of LP programming, which is the focus of this paper. Therefore, based on the work in [30], we established a linearization method of large-scale hydro-thermal SCUC. Our contributions can be summarized as follows:

(i) We establish an LP model for hydrothermal scheduling. The model of the thermal unit is linearized by the convex hull formulation. Further, we propose a linearization method for the single-UC of a hydro unit (common hydro unit and pump storage station) with variable-head units. To reduce the model size, a strategy of embedding two types of convex hulls in a multi-UC is designed. We properly choose different convex hull formulations for different units.

(ii) For the error caused by linearization, we design an efficient heuristic method to construct a feasible and near-optimal solution to the original MILP model with the optimal solution of our proposed LP model. It is proved that the error of our proposed LP model is theoretically smaller than that of the traditional LR model. In addition, the real-life case study indicates that the computational efficiency of the proposed LP model is more than twice faster than that of the LR model, and 10-100 times faster than that of the MILP model. It realizes the transformation of SCUC from the MILP model to the relaxed LP model, leading to practical large-scale uses.

II. LP MODEL OF THE SINGLE-UC WITH ONE PUMP STORAGE

In this section, according to the convex hull for single-UC with a thermal unit, we propose the MILP model for the single-UC with one pump storage and reformulate the MILP model into an LP model.

A. The model of single-UC for a thermal unit

1) The MILP model of single-UC for a thermal unit

For a single thermal unit, the corresponding MILP model can be expressed as follows:

$$\mathcal{F}^{\mathrm{MIP}} = \min \sum_{t=1}^{T} (C^{\mathrm{start}} u_t + C^{\mathrm{shut}} (u_t + x_{t-1} - x_t) + f_t(P_t, x_t)) \quad (1)$$

$$s.t. \quad x_t - x_{t-1} \le u_t,\ t \in [1,T]_{\mathbb{Z}} \quad (2)$$

$$x_t P^{\min} \le P_t \le x_t P^{\max},\ t \in [1,T]_{\mathbb{Z}} \quad (3)$$

$$\sum_{i=t-T^{\mathrm{on}}+1}^{t} u_i \le x_t,\ t \in [T^{\mathrm{on}}, T]_{\mathbb{Z}} \quad (4)$$

$$\sum_{i=t-T^{\mathrm{off}}+1}^{t} u_i \le 1 - x_{t-T^{\mathrm{off}}},\ t \in [T^{\mathrm{off}}, T]_{\mathbb{Z}} \quad (5)$$

$$\left| P_t - P_{t-1} \right| \le R^1 x_{t-1} + R^0 (1 - x_{t-1}),\ t \in [1,T]_{\mathbb{Z}} \quad (6)$$

$$x_0 = 0, u_0 = 0,\ \ x_t, u_t \in \{0,1\},\ C^{\mathrm{start}} \ge 0, C^{\mathrm{shut}} \ge 0 \quad (7)$$

The objective function (1) is to minimize the total operating cost, including generation cost and generators' start-up/shut-down cost, and specifically $f_t(P_t, x_t)$ represents the fuel cost minus the revenue and is approximated by a piece-wise linear function. Constraint (2) denotes the logical relationship between the binary variables x_t and u_t. Constraint (3) limits the generation output. Constraints (4)-(5) restrict the minimum-up/-down time to avoid frequent start-up and shut-down. Constraint (6) specifies the ramp-up/-down rate limits. Constraint (7) specifies the range of decision variables and the initial state of the unit.

2) The convex hull for the single-UC with a thermal unit

As shown in Fig.1, the convex hull is the tightest convex relaxation of an MILP model. Ref. [30] provided two convex hulls in high dimensions for the MILP model of single-UC. For convenience, the two convex hulls are named $\mathcal{G}$ -convex hull and $\mathcal{E}$- convex hull, respectively. Through the convex hull, the discrete feasible region of the single-UC for a thermal unit is transformed into a convex polyhedron formed by linear constraints, and the MILP model will be equivalent to an LP. The feasible region can be represented as

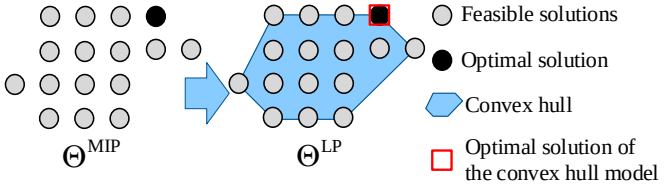

Fig.1 Convex hull of single-UC

$$\Theta^{\mathrm{MIP}} = \{(\mathbf{P}, \mathbf{x}, \mathbf{u}) \in \mathbb{R}^T \times \mathbb{B}^{2T} \mid (2)-(7)\} \quad (8)$$

$$\Theta^{\mathrm{LP}} = \{(\mathbf{P}, \mathbf{x}, \mathbf{u}) \in \mathbb{R}^{3T} \mid \mathbf{conv}(\Theta^{\mathrm{MILP}})\} \quad (9)$$

where **conv**(*) denotes the convex hull of a set *, and **P**, **x**, **u** are the vector forms of P_t, x_t, u_t,$t \in [1,T]_{\mathbb{Z}}$, respectively.

Specifically, the $\mathcal{G}$ -convex hull is formed on the set $\mathcal{G}$ which contains all the possible "on" intervals as shown below:

$$\mathcal{G}=\{(t,k)\,|\,t\in[1,T]_{\mathbb{Z}},k\in[\min\{t+T^{on}-1,T\},T]\} \quad (10)$$

The $\mathcal{G}$ -convex hull can be represented as

$$\mathcal{F}_{\mathrm{LP}}^{\mathcal{G}}=\min\sum_{t=1}^{T}(C^{\mathrm{start}}u_t+C^{\mathrm{shut}}(u_t+x_{t-1}-x_t)+f_t(P_t,x_t)) \quad (11)$$

$$s.t. \quad P_\tau=\sum_{(t,k)\in\mathcal{G},\tau\in[t,k]_{\mathbb{Z}}}\rho_{t,k}^{\tau},\tau\in[1,T]_{\mathbb{Z}} \quad (12)$$

$$x_\tau=\sum_{(t,k)\in\mathcal{G},\tau\in[t,k]_{\mathbb{Z}}}\beta_{t,k},\tau\in[1,T]_{\mathbb{Z}} \quad (13)$$

$$u_\tau=\alpha_\tau+\sum_{(t,k)\in\mathcal{G},k=\tau}\gamma_{t,k},\tau\in[1,T]_{\mathbb{Z}} \quad (14)$$

$$\sum_{t\in[1,T]_{\mathbb{Z}}}\alpha_t\le 1 \quad (15)$$

$$\alpha_t=\sum_{k=[\min\{t+T^{\mathrm{on}}-1,T\},T]}\beta_{t,k}-\sum_{k=[T^{\mathrm{on}},t-T^{\mathrm{off}}-1]_{\mathbb{Z}}}\gamma_{k,t},t\in[1,T]_{\mathbb{Z}} \quad (16)$$

$$-\sum_{k=[1,t-T^{\mathrm{on}}+1]_{\mathbb{Z}}}\beta_{k,t}+\sum_{k=[t+T^{\mathrm{off}}+1,T]_{\mathbb{Z}}}\gamma_{t,k}\le 0,t\in[T^{\mathrm{on}},T-T^{\mathrm{off}}-1]_{\mathbb{Z}} \quad (17)$$

$$\chi_t-\sum_{k=[1,t-T^{\mathrm{on}}+1]_{\mathbb{Z}}}\beta_{k,t}=0,t\in[T-T^{\mathrm{off}},T]_{\mathbb{Z}} \quad (18)$$

$$\beta_{t,k}P^{\min}\le\rho_{t,k}^{\tau}\le\beta_{t,k}P^{\max},\tau\in[t,k]_{\mathbb{Z}},(t,k)\in\mathcal{G} \quad (19)$$

$$\rho_{t,k}^{t}\le R^0\beta_{t,k},\rho_{t,k}^{k}\le R^0\beta_{t,k},(t,k)\in\mathcal{G} \quad (20)$$

$$-R^1\beta_{t,k}\le\rho_{t,k}^{\tau}-\rho_{t,k}^{\tau\text{-}1}\le R^1\beta_{t,k},\tau\in[t+1,k],(t,k)\in\mathcal{G} \quad (21)$$

$$\alpha,\beta,\gamma,\chi\ge 0 \quad (22)$$

A total of $3|\mathcal{G}|+5T$ variables are required to form a $\mathcal{G}$ -convex hull. The computational complexity of the above LP model is $O(T^2)$, and the $\mathcal{G}$ -convex hull is equivalent to the original MILP model. The feasible region of the single-UC by $\mathcal{G}$ -convex hull can be represented as

$$\Theta_{\mathcal{G}}^{\mathrm{LP}}=\{(\mathbf{P},\mathbf{x},\mathbf{u},\boldsymbol{\alpha},\boldsymbol{\beta},\boldsymbol{\chi},\boldsymbol{\gamma})\in\mathbb{R}^{3|\mathcal{G}|+5T}\,|\,((12)\text{-}(22))\} \quad (23)$$

The $\mathcal{E}$ -convex hull is formed on the set $\mathcal{E}$ which contains all the possible optimal generation amounts and on/off statuses. The $\mathcal{E}$ -convex hull can be represented as follows:

$$\mathcal{F}_{\mathrm{LP}}^{\mathcal{E}}=\min\sum_{t\in[1,T]_{\mathbb{Z}}}[C^{\mathrm{start}}u_t+C^{\mathrm{shut}}(x_{t-1}-x_t+u_t)+f_t(P_t,x_t)] \quad (24)$$

s.t.

$$P_t=\sum_{e_i\in\mathcal{E},e_j\in\Gamma_{i\Rightarrow}}P(e_j)\lambda_{tij} \quad (25)$$

$$x_t=\sum_{e_i\in\mathcal{E},e_j\in\Gamma_{i\Rightarrow}}x(e_j)\lambda_{tij} \quad (26)$$

$$u_t=\sum_{e_i\in\mathcal{E},e_j\in\Gamma_{i\Rightarrow}}u(e_j)\lambda_{tij} \quad (27)$$

$$\sum_{e_j\in\Gamma_{1\Rightarrow}}\lambda_{11j}=1 \quad (28)$$

$$\sum_{e_j\in\Gamma_{i\Rightarrow}}\lambda_{1ij}=0,e_i\in\mathcal{E}\setminus\mathcal{E}_0 \quad (29)$$

$$\sum_{e_j\in\Gamma_{i\Rightarrow}}\lambda_{tij}-\sum_{e_k\in\Gamma_{\Rightarrow i}}\lambda_{t-1,ki}=0,e_i\in\mathcal{E},t\in[2,T]_{\mathbb{Z}} \quad (30)$$

$$\lambda_{tij}\ge 0,\ \ e_i\in\mathcal{E},e_j\in\Gamma_{i\Rightarrow},t\in[1,T]_{\mathbb{Z}} \quad (31)$$

where $P(e_j)$, $x(e_j)$, and $u(e_j)$ denote the generation amount, on/off status, and start-up status if the optimal state of the generator is e_j at time t, respectively. $P(e_j)$, $x(e_j)$, and $u(e_j)$ are presolved parameters determined by the optimal state e_j, the construction details are given in [30]. A total of $3T+|\mathcal{E}||\mathcal{Q}|T$ variables are required to form a $\mathcal{E}$ convex hull, the dimension of set $|\mathcal{E}|$ and the set $|\mathcal{Q}|$ are clarified in III.B. The computational complexity of the above LP model is $O(|\mathcal{E}||\mathcal{Q}|T)$, and the feasible region of the single-UC by $\mathcal{E}$ -convex hull can be represented as follows:

$$\Theta_{\mathcal{E}}^{\mathrm{LP}}=\{(\mathbf{P},\mathbf{x},\mathbf{u},\boldsymbol{\lambda})\in\mathbb{R}^{|Q||\mathcal{E}|T+3T}\,|\,(25)\text{-}(31)\}. \quad (32)$$

Although the $\mathcal{G}$ -convex hull and the $\mathcal{E}$ -convex hull are constructed with different variables, the optimal solutions $\mathbf{P}^*,\mathbf{x}^*,\mathbf{u}^*$ of the single-UC with the two convex hulls are the same. Therefore, both the $\mathcal{G}$ -convex hull and the $\mathcal{E}$ -convex hull can be regarded as the convex hull of the original MILP problem. Note that the convex hull of the single-UC model with a thermal unit is related to only the physical parameters of the unit but not the load and network topology, so it can be modeled offline and only once.

B. The model for the single-UC with one pump storage

1) The MILP model for the single-UC with one pump storage

A pump storage station, which consists of an upstream reservoir, a downstream reservoir, a hydro generator, and a pump, can either absorb or generate electricity. The pump storage station can undertake the tasks of peak load shifting in the power systems, releasing water from the upstream to downstream reservoirs to generate electricity by the hydro generator during peak load, and pumping water from the downstream to upstream reservoirs by the pump to consume electricity during valley loads. A pump storage station has three possible statuses: pumping, generating, and shutdown, and can be operated in only one of these statuses at any time.

For a pump storage station, both unit constraints and reservoir constraints should be considered.

The reservoir constraints include:

$$V^{\mathrm{up,min}}\le V_t^{\mathrm{up}}\le V^{\mathrm{up,max}},V^{\mathrm{dn,min}}\le V_t^{\mathrm{dn}}\le V^{\mathrm{dn,max}} \quad (33)$$

$$\begin{aligned}V_{t+1}^{\mathrm{up}}-V_t^{\mathrm{up}}&=W_t^{\mathrm{pump}}-W_t^{\mathrm{hydro}}+U_t^{\mathrm{up}}\\ V_{t+1}^{\mathrm{dn}}-V_t^{\mathrm{dn}}&=W_t^{\mathrm{hydro}}-W_t^{\mathrm{pump}}+U_t^{\mathrm{dn}},\end{aligned} \quad (34)$$

where constraint (33) provides the upper and lower bounds of the reservoir volume. Constraint (34) represents the reservoir volume balance considering the natural inflow.

The unit constraints include:

$$x_t-x_{t-1}\le u_t,t\in[1,T]_{\mathbb{Z}} \quad (35)$$

$$z_t+x_t\le 1,t\in[1,T]_{\mathbb{Z}} \quad (36)$$

$$\sum_{i=t-T^{\mathrm{on}}+1}^{t}u_i\le x_t,t\in[T^{\mathrm{on}},T]_{\mathbb{Z}} \quad (37)$$

$$\sum_{i=t-T^{\mathrm{off}}+1}^{t}u_i\le 1-x_{t-T^{\mathrm{off}}},t\in[T^{\mathrm{off}},T]_{\mathbb{Z}} \quad (38)$$

$$x_tP^{\mathrm{hydro,min}}\le P_t^{\mathrm{hydro}}\le x_tP^{\mathrm{hydro,max}},t\in[1,T]_{\mathbb{Z}} \quad (39)$$

$$z_tP^{\mathrm{pump,min}}\le P_t^{\mathrm{pump}}\le z_tP^{\mathrm{pump,max}},t\in[1,T]_{\mathbb{Z}} \quad (40)$$

$$\left|P_t^1-P_{t-1}^1\right|\le R^1x_{t-1}+R^0(1-x_{t-1}),t\in[1,T]_{\mathbb{Z}} \quad (41)$$

$$P_t=P_t^{\mathrm{hydro}}-P_t^{\mathrm{pump}},t\in[1,T]_{\mathbb{Z}} \quad (42)$$

$$P_t^{\mathrm{hydro}}=\eta^{\mathrm{w\text{-}e}}W_t^{\mathrm{hydro}}h_t^{\mathrm{up}},t\in[1,T]_{\mathbb{Z}} \quad (43)$$

$$h_t^{\mathrm{up}}=\psi_1\left(V_t^{\mathrm{up}}\right),t\in[1,T]_{\mathbb{Z}} \quad (44)$$

$$P_t^{\mathrm{pump}}=\eta^{\mathrm{e\text{-}w}}W_t^{\mathrm{pump}}h_t^{\mathrm{dn}},t\in[1,T]_{\mathbb{Z}} \quad (45)$$

$$h_t^{\mathrm{dn}} = \psi_2\left(V_t^{\mathrm{dn}}\right), t \in [1,T]_{\mathbb{Z}} \tag{46}$$

where constraints (35)-(36) limit the operation status of the pump storage station. Constraints (37)-(38) restrict the minimum-up/-down periods. Constraints (39)-(40) denote the limits on water consumption and pumping capacity. Constraint (41) specifies the ramp-up/-down rate limits of the hydro unit. Constraints (42)-(46) describe the conversion relationship between water consumption and power generation with a variable water head, which is highly nonlinear.

The nonlinear function (44) and (46) can be handled by the piecewise linearization method [35]. Besides, (43) and (45) are bilinear constraints. They can be linearized by constructing a convex envelope around the bilinear relationship, such as McCormick's envelopes (e.g., [36]). Constraint (43) can be linearized as:

$$\begin{aligned}
&P_t^{\mathrm{hydro}} \geq \eta^{\mathrm{w\text{-}e}}(W_t^{\mathrm{hydro,min}} h_t^{\mathrm{up}} + W_t^{\mathrm{hydro}} h_t^{\mathrm{up,min}} - W_t^{\mathrm{hydro,min}} h_t^{\mathrm{up,min}}) \\
&P_t^{\mathrm{hydro}} \geq \eta^{\mathrm{w\text{-}e}}(W_t^{\mathrm{hydro,max}} h_t^{\mathrm{up}} + W_t^{\mathrm{hydro}} h_t^{\mathrm{up,max}} - W_t^{\mathrm{hydro,max}} h_t^{\mathrm{up,max}}) \\
&P_t^{\mathrm{hydro}} \leq \eta^{\mathrm{w\text{-}e}}(W_t^{\mathrm{hydro,min}} h_t^{\mathrm{up}} + W_t^{\mathrm{hydro}} h_t^{\mathrm{up,max}} - W_t^{\mathrm{hydro,min}} h_t^{\mathrm{up,max}}) \\
&P_t^{\mathrm{hydro}} \leq \eta^{\mathrm{w\text{-}e}}(W_t^{\mathrm{hydro,max}} h_t^{\mathrm{up}} + W_t^{\mathrm{hydro}} h_t^{\mathrm{up,min}} - W_t^{\mathrm{hydro,max}} h_t^{\mathrm{up,min}})
\end{aligned} \tag{47}$$

$$\begin{aligned}
&P_t^{\mathrm{pump}} \geq \eta^{\mathrm{e\text{-}w}}(W_t^{\mathrm{pump,min}} h_t^{\mathrm{dn}} + W_t^{\mathrm{pump}} h_t^{\mathrm{dn,min}} - W_t^{\mathrm{pump,min}} h_t^{\mathrm{dn,min}}) \\
&P_t^{\mathrm{pump}} \geq \eta^{\mathrm{e\text{-}w}}(W_t^{\mathrm{pump,max}} h_t^{\mathrm{dn}} + W_t^{\mathrm{pump}} h_t^{\mathrm{dn,max}} - W_t^{\mathrm{pump,max}} h_t^{\mathrm{dn,max}}) \\
&P_t^{\mathrm{pump}} \leq \eta^{\mathrm{e\text{-}w}}(W_t^{\mathrm{pump,min}} h_t^{\mathrm{dn}} + W_t^{\mathrm{pump}} h_t^{\mathrm{dn,max}} - W_t^{\mathrm{pump,min}} h_t^{\mathrm{dn,max}}) \\
&P_t^{\mathrm{pump}} \leq \eta^{\mathrm{e\text{-}w}}(W_t^{\mathrm{pump,max}} h_t^{\mathrm{dn}} + W_t^{\mathrm{pump}} h_t^{\mathrm{dn,min}} - W_t^{\mathrm{pump,max}} h_t^{\mathrm{dn,min}})
\end{aligned} \tag{48}$$

Since the hydro units work without fuel consumption, only the startup/shutdown costs and maintenance costs (i.e., f_t) need to be considered in the objective function. Hence, the MILP model of pump storage single-UC can be expressed as follows:

$$\min_{(\mathbf{P},\mathbf{x},\mathbf{z},\mathbf{u},\mathbf{v})\in\Psi^{\mathrm{MIP}}} \sum_{t=1}^{T} (C^{\mathrm{start}} u_t + C^{\mathrm{shut}}(u_t + x_{t-1} - x_t) + f_t(P_t, x_t, z_t)) \tag{49}$$

$$\Psi^{\mathrm{MILP}} = \{ (\mathbf{P}^{\mathrm{hydro}}, \mathbf{P}^{\mathrm{pump}}, \mathbf{x}, \mathbf{z}, \mathbf{u}, \mathbf{v}) \mid (33)\text{-}(48) \} \tag{50}$$

where $\mathbf{P}^{\mathrm{hydro}}$, $\mathbf{P}^{\mathrm{pump}}$, $\mathbf{z}$, $\mathbf{v}$ are the vector forms of P_t^{hydro}, P_t^{pump}, z_t, v_t,$t\in[1,T]_{\mathbb{Z}}$, respectively.

2) The LP model for the single-UC with one pump storage

It is challenging to directly establish the convex hull for the single-UC with one pump storage as that with a thermal unit. The reasons are presented as follows:

First, the $\mathcal{E}$ -convex hull is constructed with all the possible optimal generation amounts. For a thermal unit that can be regarded as a closed system, the optimal state space is only dependent on the unit's inherent parameters, and we can use the convex hull under any external parameter. In contrast, the optimal states of a pump storage station are affected by the external continuous natural inflow, which leads to the non-generality that the constructed convex hull is only applicable to a given natural flow. Therefore, the $\mathcal{E}$ -convex hull is not directly applicable for the pump storage.

Second, the $\mathcal{G}$ -convex hull is established with all the possible "on" intervals, and the operating cost for each "on" interval needs to be pre-solved. For any given interval $[t,k]_{\mathbb{Z}}$, the operating cost of a thermal unit is independent of the on/off status before time *t*. In contrast, the reservoir volume at different time periods is coupled with water consumption. Different statuses before time *t* will lead to different initial reservoir volume status and operating costs in the interval $[t,k]_{\mathbb{Z}}$. As a result, the $\mathcal{G}$ -convex hull cannot be directly applied to the pump storage.

To address this problem, we model the hydro generator and the pump as two separate thermal units, where one is with positive power outputs and the other is with negative power outputs, respectively. Therefore, pump storage can be equivalent to two coupled thermal units with positive power outputs P_t^{hydro} and negative power outputs -P_t^{pump}.

The feasible region of the unit with the positive power (i.e., the hydro generator) can be expressed as follows:

$$\Psi^{\mathrm{hydro,MILP}} = \{ (\mathbf{P}^{\mathrm{hydro}}, \mathbf{x}, \mathbf{u}) \in \mathbb{R}^T \times \mathbb{B}^{2T} \mid (35),(37)\text{-}(39),(41) \} \tag{51}$$

which is the same as the MILP model with thermal units. In particular, (35) corresponds to (2), (39) corresponds to (3), (37) and (38) correspond to (4) and (5), and (41) corresponds to (6). Therefore, the convex hull of the MILP can be formed by

$$\Psi^{\mathrm{hydro,LP}} = \{ (\mathbf{P}^{\mathrm{hydro}}, \mathbf{x}, \mathbf{u}) \in \mathbb{R}^{3T} \mid \Theta_{\Lambda}^{\mathrm{LP}}, \Lambda = \mathcal{G} \text{ or } \mathcal{E} \} \tag{52}$$

Meanwhile, the feasible region of the unit with the negative power (i.e., the pump) can be expressed as follows:

$$\Psi^{\mathrm{pump,MILP}} = \{ (\mathbf{P}^{\mathrm{pump}}, \mathbf{z}) \in \mathbb{R}^T \times \mathbb{B}^T \mid (40) \} \tag{53}$$

which is not the same as the MILP model with thermal units. To take advantage of the convex hull, we introduce one redundant variable v_t and four redundant constraints as follows:

$$z_t - z_{t-1} \leq v_t, t \in [1,T]_{\mathbb{Z}} \tag{54}$$

$$u_t \leq x_t, t \in [1,T]_{\mathbb{Z}} \tag{55}$$

$$u_t \leq 1 - x_{t-1}, t \in [2,T]_{\mathbb{Z}} \tag{56}$$

$$\left| P_t^{\mathrm{pump}} - P_{t-1}^{\mathrm{pump}} \right| \leq \eta^{\mathrm{e\text{-}w}} W^{\mathrm{pump,max}} \psi_2(V^{\mathrm{dn,max}}), t \in [1,T]_{\mathbb{Z}} \tag{57}$$

where constraint (54) limits the operation status of the pump, constraints (55)-(56) indicate that any status of the unit should continue for at least one period. Constraint (57) describes the ramp-up/-down rate limits. Clearly, redundant constraints do not change the feasible region of the pump, which can be reformulated as follows:

$$\Psi^{\mathrm{pump,MILP}} = \{ (\mathbf{P}^{\mathrm{pump}}, \mathbf{z}, \mathbf{v}) \in \mathbb{R}^T \times \mathbb{B}^{2T} \mid (40),(54)\text{-}(57) \} \tag{58}$$

Although the above model is more complex, $\Psi^{\mathrm{pump,MILP}}$ has a similar form as the MILP model with thermal units. In particular, (54) corresponds to (2), (40) corresponds to (3), (55) and (56) correspond to (4) and (5), and (57) corresponds to (6). Therefore, $\Psi^{\mathrm{pump,LP}}$ can be formed as below:

$$\Psi^{\mathrm{pump,LP}} = \{ (\mathbf{P}^{\mathrm{pump}}, \mathbf{z}, \mathbf{v}) \in \mathbb{R}^{3T} \mid \Theta_{\Lambda}^{\mathrm{LP}}, \Lambda = \mathcal{G} \text{ or } \mathcal{E} \} \tag{59}$$

Finally, according to (52) and (59), the single-UC with a pump storage station can be solved by a relaxed LP model whose formulation can be expressed as

$$\Psi^{\mathrm{LP}} = \{ (\mathbf{P}, \mathbf{x}, \mathbf{z}, \mathbf{u}, \mathbf{v}) \in \mathbb{R}^{5T} \mid \Psi^{\mathrm{hydro,LP}}, \Psi^{\mathrm{pump,LP}}, \{(33)\text{-}(34),(42)\text{-}(48)\} \} \tag{60}$$

The proposed LP formulation (60) does not represent the convex hull of the feasible region but provides a relaxed LP model. The numerical experiment in Section IV.B suggests that the relaxation error is very small. In addition, the proposed method can also model the common hydro, which can be modeled as one thermal power unit and its reservoir constraints. For the power system with cascaded plants, an LP model can be similarly established by using the convex hull formulation of a

single-UC, though its performance may not meet the economic requirements. In summary, the proposed model is suitable for the hydrothermal unit commitment problem with decoupled thermal units and variable-head hydro units.

III. LP MODEL OF THE MULTI-UC FOR HYDROTHERMAL SCHEDULING

In this section, we first propose the LP model of the multi-UC for hydrothermal scheduling, and then design the strategy of embedding two types of convex hulls in the multi-UC and the method of recovering a feasible solution. Finally, we analyze the error of the proposed LP model.

A. The model of the multi-UC for hydrothermal scheduling

1) The MILP model of the multi-UC

The multi-UC model can be expressed as (61)-(66) in the following formulation.

$$\mathcal{L}=\min \sum_{t=[1,T]_{\mathbb{Z}}} \sum_{g\in G\bigcup H} (C_{g,t}^{\text{start}} u_{g,t} + C_{g,t}^{\text{shut}} (u_{g,t} + x_{g,t-1} - x_{g,t}) + f_{g,t}(P_{g,t}, x_{g,t})) \tag{61}$$

$$(\mathbf{P_g}, \mathbf{x_g}, \mathbf{u_g}) \in \Theta_g^{\text{MILP}}, g \in G, t \in [1,T]_{\mathbb{Z}} \tag{62}$$

$$(\mathbf{P_g}, \mathbf{x_g}, \mathbf{z_g}, \mathbf{u_g}, \mathbf{v_g}) \in \Psi_g^{\text{MILP}}, g \in H, t \in [1,T]_{\mathbb{Z}} \tag{63}$$

$$\sum_{g\in G\cup H} P_{g,t} = \sum_{b\in Bus} D_{b,t}, t \in [1,T]_{\mathbb{Z}} \tag{64}$$

$$\sum_{g\in G} P_g^{\max} x_g \geq \sum_{b\in Bus} D_{b,t} + r_t, t \in [1,T]_{\mathbb{Z}} \tag{65}$$

$$\left| \sum_{g\in G\bigcup H} H_l^{\text{PTDF}} C_g P_{g,t} - \sum_{b\in Bus} H_{l,b}^{\text{PTDF}} D_{b,t} \right| \leq F_l^{\max}, l \in L, t \in [1,T]_{\mathbb{Z}} \tag{66}$$

where $\mathbf{P}_g$,$\mathbf{x}_g$,$\mathbf{z}_g$,$\mathbf{u}_g$,$\mathbf{v}_g$ are the vector forms of $P_{g,t}$, $x_{g,t}$, $z_{g,t}$, $v_{g,t}$, $t\in[1,T]_{\mathbb{Z}}$. The objective function (61) is to minimize the total operating cost, subject to the physical constraints (62)-(63) of units, the power balance constraint (64), reserve constraint (65), and transmission capacity constraint (66).

2) The LP model of multi-UC

Note that integer variables only exist in constraints (61)-(62). Replacing the constraints (61)-(62) with the convex hull of each unit gives the following formulation:

$$\mathcal{L}=\min \sum_{t=[1,T]_{\mathbb{Z}}} \sum_{g\in G\cup H} \begin{matrix}(C_{g,t}^{\text{start}} u_{g,t} + C_{g,t}^{\text{shut}} (u_{g,t} + x_{g,t-1} - x_{g,t}) \\ + f_{g,t}(P_{g,t}, x_{g,t}))\end{matrix} \tag{67}$$

$$\text{s.t. } (\mathbf{P_g}, \mathbf{x_g}, \mathbf{u_g}) \in \Theta_{\Lambda,g}^{\text{LP}}, g \in G, t \in [1,T]_{\mathbb{Z}}, \Lambda = \mathcal{E} \text{ or } \mathcal{G} \tag{68}$$

$$(\mathbf{P_g}, \mathbf{x_g}, \mathbf{u_g}) \in \Psi_g^{\text{LP}}, g \in H, t \in [1,T]_{\mathbb{Z}} \tag{69}$$

$$(64)\text{-}(66) \tag{70}$$

The above formulation transforms the original MILP model into an LP model ($u_{g,t}$ and $x_{g,t}$ are defined as continuous variables) with a relaxed feasible region. However, there are still three problems to quickly obtaining a high-quality feasible solution of the multi-UC model.

1) Although the single-UC model can be formulated as an LP by either $\mathcal{E}$-convex hull or $\mathcal{G}$-convex hull, the two convex hulls have different computational complexity. The poor adaptability of a unit to a convex hull often leads to an overall slowdown or even insolvability. Therefore, how to properly choose the form of a convex hull is quite crucial.

2) Fig.2(a) shows the framework of the multi-UC model, containing several convex hulls of each single-UC model and the coupling constraints (i.e., system constraints (64)-(66) and reservoir constraints (33)-(34) of hydropower units). In Fig.2(b), compared with the convex hull of the multi-UC (the blue area), the formulation (67)-(70) provides a relaxed feasible region (the yellow area), which may induce a fractional optimal solution because the extreme points of this formulation may not be binary. Therefore, it is necessary to design a method to recover an integer feasible solution near the extreme points.

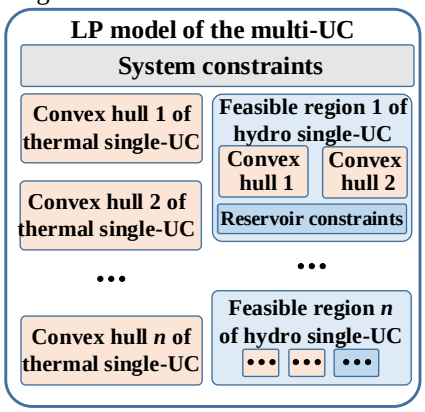

(a) Framework of the LP

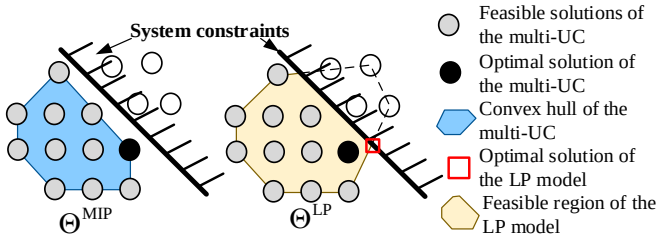

(b) Relaxed polyhedral feasible region

Fig.2 The LP model of multi-UC

3) The recovered feasible solution may not be an optimal solution. The error upper bound between the feasible suboptimal solution of the LP model and the optimal solution of the original MILP model should be determined. We theoretically prove that the optimal solution of the proposed LP model is better than the optimal solution of the LR model, providing an upper bound for the error.

B. The strategy of embedding two types of convex hulls in the multi-UC

Note that the computational complexity of the $\mathcal{E}$-convex hull is $O(|\mathcal{Q}||\mathcal{E}|\ T)$. $\mathcal{Q}$ is the set of all the possible optimal generation levels under different conditions, which can be proved to be discrete in [30] as follows

$$\mathcal{Q}=\{0,(P^{\min}+nR^1)_{n=0}^{n_1},(R^0+nR^1)_{n=0}^{n_2},(P^{\max}-nR^1)_{n=0}^{n_1}\} \tag{71}$$

where n_1=max{$t\in[1,T]_{\mathbb{Z}}|P^{\min}+nR^1\leq P^{\max}$}, n_2=max{$t\in[1,T]_{\mathbb{Z}}|$ $R^0+nR^1\leq P^{\max}$}. Therefore, $|\mathcal{Q}|$ is at most $2n_1+n_2+1$, which can be represented as

$$|\mathcal{Q}|\leq 2n_1+n_2+1=2\left\lfloor \frac{P^{\max}-P^{\min}}{R^1} \right\rfloor+\left\lfloor \frac{P^{\max}-R^0}{R^1} \right\rfloor+1 \tag{72}$$

where $\lfloor * \rfloor$ denotes the largest integer number no larger than *. $\mathcal{E}$ is the set containing all the states when the generator is offline or online. The number of offline states is T^{off}, and the

number of online states is $|\mathcal{Q}|T^{\text{on}}$ [30]. $\mathcal{E}$ is a finite set and the dimension of the set $\mathcal{E}$ is $|\mathcal{Q}|T^{\text{on}}+T^{\text{off}}$.

Once T is fixed, the computational complexity of the $\mathcal{E}$-convex hull is only related to the unit inherent parameters, i.e., R^1, R^0, T^{on}, and T^{off}. Therefore, $\mathcal{E}$-convex hull can be suitable for the units with large R^1, R^0, or small T^{on}, T^{off}, such as gas-fired and oil-fired units.

The computational complexity of the $\mathcal{G}$-convex hull is $O(T^2)$. According to the definition of $\mathcal{G}$, the number of elements can be expressed as below:

$$|\mathcal{G}|=\sum_{n=1}^{(T-T^{\text{on}})} n=\frac{1}{2}(T-T^{\text{on}})(T-T^{\text{on}}+1)\approx\frac{1}{2}(T-T^{\text{on}})^2 \quad (73)$$

It is observed from (12)-(22) that the $\mathcal{G}$-convex hull is constructed by $3T+4|\mathcal{G}|$ constraints and $5T+3|\mathcal{G}|$ decision variables. Once T is fixed, the complexity of the convex hull is only related to T^{on}. As T^{on} increases, $|\mathcal{G}|$ decreases. For example, when $T^{\text{on}}=T$, the possible operating states of the unit are reduced to two, i.e., on or off for the entire scheduling horizon. In this case, only $3T + 4$ constraints and $5T + 3$ variables are needed to characterize the feasible region of a unit. In a real-life power system, the unit with a long T^{on} is usually the large thermal unit. This is because the startup and shutdown of the thermal unit are realized by the boiler and steam turbine. Frequent startup and shutdown of the boiler will damage the boiler pipe joint, resulting in shaft bending and reducing the service life. Therefore, the $\mathcal{G}$-convex hull can be suitable for the units with long T^{on}, such as thermal units.

In addition, when the physical parameters of all the units are given, the computational complexity of the $\mathcal{G}$-convex hull is $O(T^2)$, and that of the $\mathcal{E}$-convex hull is $O(T)$. Therefore, the $\mathcal{G}$-convex hull is not suitable for the long-timescale unit commitment, while the $\mathcal{E}$-convex hull can have an excellent performance in long-timescale multi-UC.

From the above analysis, the two convex hulls clearly differ from each other in terms of computational complexity and application scenarios. For some dispatchable units, properly choosing a form of the convex hull is very important to improve the solution efficiency. For example, for the unit satisfying $R^1<<P^{\max}-P^{\min}$, it would be better to choose the $\mathcal{G}$-convex hull.

To address the problem of properly choosing the form of a convex hull, we propose the strategy of embedding two types of convex hulls in the multi-UC by comparing the number of decision variables required to form the two convex hulls. Constructing a $\mathcal{G}$-convex hull requires $3|\mathcal{G}|+5T$ decision variables and constructing a $\mathcal{E}$-convex hull requires $|\mathcal{Q}|(|\mathcal{Q}|T^{\text{on}}+T^{\text{off}})T+3T$ variables. We select the convex hull form with fewer variables. This process is implemented by

$$\Theta^{\text{LP}}=\begin{cases}\Theta_{\mathcal{E}}^{\text{LP}}, |\mathcal{Q}|(|\mathcal{Q}|T^{\text{on}}+T^{\text{off}})T\le 3|\mathcal{G}|+2T\\ \Theta_{\mathcal{G}}^{\text{LP}}, |\mathcal{Q}|(|\mathcal{Q}|T^{\text{on}}+T^{\text{off}})T> 3|\mathcal{G}|+2T\end{cases} \quad (74)$$

Since $|\mathcal{Q}|$ is related to R^1, the parameters (i.e., R^1, T^{on}, and T^{off}) are inherent properties of the units and are not related to network, load, etc. Then, (74) can be computed offline without additional solution time. The strategy improves the overall computational efficiency by using different convex hulls for different units to construct the multi-UC model. The scale of the corresponding LP model is smaller than that using only one type of convex hull. In addition, the $\mathcal{G}$-convex hull and the $\mathcal{E}$-convex hull are both the tightest formulation of a single-UC. When constructing the feasible region of the generators, it's equivalent to selecting the $\mathcal{G}$-convex hull or the $\mathcal{E}$-convex hull in terms of the optimal value.

C. The method of recovering a feasible solution

The proposed method is different from the standard method that has been used in the Lagrangian relaxation literature [33]-[34], which used dual information (e.g., the opportunity cost) to adjust the unit status period by period. The proposed method is to find an integer feasible and near-optimal solution based on an optimal solution from the relaxed feasible region given by formulation (67)-(70). Specifically, the optimal solution $x_{g,t}^*$ is a $(|G|+|H|)T$-dimensional vector in which few dimensions are fractional. We first adjust these fractional numbers to be integers and then determine whether the modified solution is feasible. The detailed steps are described as follows:

Step1. As $\mathbf{x}\in[0,1]_{\text{R}}$, there are three possible values of $x_{g,t}^*$ (Optimal solution of $x_{g,t}$), which are $x_{g,t}^*=0$, $x_{g,t}^*=1$, $0< x_{g,t}^* <1$, respectively. Thus, all the generators associated with different time periods can be divided into three disjoint sets as follows:

$$\begin{aligned}\Omega_{0,1}&=\{(g,t)\,|\,x_{g,t}^*=0\vee x_{g,t}^*=1,\forall t,\forall g\}\\ \Omega_{0,\varepsilon}&=\{(g,t)\,|\,|1-x_{g,t}^*|<0.5,\forall t,\forall g\}\\ \Omega_{\varepsilon,1}&=\{(g,t)\,|\,|0-x_{g,t}^*|\le 0.5,\forall t,\forall g\}\end{aligned} \quad (75)$$

where $\wedge$ and $\vee$ denote the logical "and" and "or," respectively.

Step2. Keep the unit status unchanged for each generator in a period in the set $\Omega_{0,1}$, and adjust the unit status in the set $\Omega_{0,\varepsilon}$ and $\Omega_{\varepsilon,1}$ as

$$x_{g,t}^*=0,\ \forall(g,t)\in\Omega_{0,\varepsilon} \quad (76)$$

$$x_{g,t}^*=1,\ \forall(g,t)\in\Omega_{\varepsilon,1} \quad (77)$$

We check whether the above solution is a feasible solution for the multi-UC model via the following necessary and sufficient conditions [33].

$$\begin{aligned}\sum_{g\in E_{1t}}P_g^{\max}+\sum_{g\in E_{2t}}P_g^{\min}\ge\sum_{b\in Bus}D_{b,t}-\sum_{g\in E_{3t}}P_g^{\min}\\ +\max\{0,r_t-\sum_{g\in E_{3t}}(P_g^{\max}-P_{g,t})x_{g,t}^*\}\end{aligned} \quad (78)$$

$$\sum_{g\in E_{1t}}(P_g^{\max}-P_{g,t})x_{g,t}^*\ge r_t-\sum_{g\in E_{3t}}(P_g^{\max}-P_{g,t})x_{g,t}^* \quad (79)$$

$$\sum_{g\in E_{1t}}P_g^{\min}+\sum_{g\in E_{2t}}P_g^{\min}\le\sum_{b\in Bus}D_{b,t}-\sum_{g\in E_{3t}}P_{g,t} \quad (80)$$

If the solution is not feasible, then turn to **step3**; if the solution is feasible, then solve the economic dispatch problem (61)-(62) with the current unit on/off status. Then, we can get the suboptimal solution of the multi-UC model and stop the iteration.

Step3. We define the scheduled unit as the unit whose statuses are binary in all periods, and the unscheduled unit as the unit that is in off-status for the entire time interval $[1,T]$ or has non-binary status in some period. Dividing all units into two sets according to the above definition, we have

$$\Phi_0 = \{g \mid (g,t) \in \Omega_{0,\varepsilon} \vee (g,t) \in \Omega_{\varepsilon,1}, \exists t\} \cup \{g \mid x^*_{g,t}=0, \forall t\}$$
$$\Phi_1 = \{g \mid (g,t) \in \Omega_{0,1}, \forall t\} \setminus \{g \mid x^*_{g,t}=0, \forall t\} \quad (81)$$

where Φ_1 is defined as the set of all scheduled units, and Φ_0 is defined as the set of unscheduled units. The outputs of scheduled units are called as the scheduled power, and the difference between the total load and the scheduled power is the unscheduled power ΔD_t which can be expressed as

$$\Delta D_t = \sum_{b \in Bus} D_{b,t} - \sum_{g \in \Phi_1} P_{g,t}, t \in [1,T]_{\mathbb{Z}} \quad (82)$$

where ΔD_t usually equals 1%~5% of the total load.

Step4. Keep the statuses and outputs of the scheduled units unchanged, and reschedule the unscheduled power ΔD_t with the units in Φ_0 by the Priority-List algorithm [38] in the polynomial-time complexity. First, calculate and sort the full-load average production costs, and then a strict priority order for units in Φ_0 can be obtained by

$$\mathbf{sort}(f_g(P_g^{\max})) \quad (83)$$

where **sort**(*) is the function order * from smallest to largest.

Second, select the top $x(x \in [0,|\Phi_0|])$ units from the priority list as the combinations at each period. Finally, modify the combinations based on the system constraints and unit physical constraints.

As a result, the suboptimal feasible solution for the unscheduled power and unscheduled units are quickly recovered. Since the unscheduled power accounts for only 1%-5% of the total load, the final suboptimal solution that we obtain usually has a small gap with respect to the true optimal solution.

D. Error analysis of the LP model of the multi-UC

For the multi-UC model, we denote the optimal value of the proposed LP model by $\mathcal{L}^*$, the optimal value of the MILP model by $\mathcal{K}^*$, and the suboptimal value obtained by constructing a feasible solution from the proposed LP model by $\overline{\mathcal{L}^*}$. These three values should satisfy

$$\mathcal{L}^* \le \mathcal{K}^* \le \overline{\mathcal{L}^*} \quad (84)$$

To describe the error of the proposed model, we define the optimal value error v, convex relaxation error v_1, and feasible solution construction error v_2, respectively, as:

$$v = \overline{\mathcal{L}^*} - \mathcal{K}^*,\ v_1 = \mathcal{K}^* - \mathcal{L}^*,\ v_2 = \overline{\mathcal{L}^*} - \mathcal{L}^* \quad (85)$$

where v reflects the precise error of the proposed LP model. However, $\mathcal{K}^*$ cannot be directly obtained, whereas $\mathcal{L}^*$ and $\overline{\mathcal{L}^*}$ are easy to obtain. Thus, v_2 is usually used to measure the error. In addition, we compare the performance of our proposed LP model with that of the traditional LR model. Specifically, to describe the error of the LR model, we define its optimal value by $Z^{\mathrm{LR}*}$, the suboptimal value obtained by constructing a feasible solution by $\overline{Z^{\mathrm{LR}*}}$, the relaxation error by v_1^{LR}, and the feasible solution construction error by v_2^{LR}, respectively, as shown in the following:

$$v_1^{\mathrm{LR}} = \mathcal{K}^* - Z^{\mathrm{LR}*},\ v_2^{\mathrm{LR}} = \overline{Z^{\mathrm{LR}*}} - Z^{\mathrm{LR}*} \quad (86)$$

The following proposition will characterize the errors of our proposed LP model.

Proposition 1. We have $Z^{\mathrm{LR}*}$, $\mathcal{L}^*$, and $\mathcal{K}^*$ satisfy

$$Z^{\mathrm{LR}*} \le \mathcal{L}^* \le \mathcal{K}^* \quad (87)$$

Therefore, v_1^{LR} and v_1 satisfy

$$v_1 \le v_1^{\mathrm{LR}} \quad (88)$$

Proof. Both the LP model (67)-(70) and the MILP model (61)-(66) can be solved by the LR approach. They use the same iterative framework, but the only difference is the feasible region of the subproblem (single-UC model), such that

$$\text{MILP: } (\mathbf{P_g}, \mathbf{x_g}, \mathbf{u_g}) \in \Theta_g^{\mathrm{MILP}}$$
$$\text{LP: } (\mathbf{P_g}, \mathbf{x_g}, \mathbf{u_g}) \in \Theta_g^{\mathrm{LP}} \quad (89)$$

Note that the single-UC subproblems under both the original MILP and the proposed LP model are equivalent because the latter provides the convex hull for the former. Therefore, the multi-UC of the LP model and the MILP model are equivalent in the context of LR. Furthermore, the optimal value solved by the LR algorithm can be served as a lower bound. Thus, we have

$$Z^{\mathrm{LR}*} \le \mathcal{L}^* \quad (90)$$

$$Z^{\mathrm{LR}*} \le \mathcal{K}^* \quad (91)$$

Taking (90) and (91) into (84) gives

$$Z^{\mathrm{LR}*} \le \mathcal{L}^* \le \mathcal{K}^* \quad (92)$$

Furthermore, we have

$$v_1 = \mathcal{K}^* - \mathcal{L}^* \le \mathcal{K}^* - Z^{\mathrm{LR}*} = v_1^{\mathrm{LR}} \quad (93)$$

(**Q.E.D.**)

Proposition 2. We have v_1 satisfies

$$v_1 \le (\max\{C_g^{\mathrm{start}}\} \cdot 2T + \max\{f_g(P_g^{\min}, 1)\} \cdot 2T^2), \forall g \quad (94)$$

Furthermore, the relative error $v_1 / \mathcal{K}^*$ satisfies

$$\lim_{n \to \infty} \frac{v_1}{\mathcal{K}^*} = \lim_{n \to \infty} \frac{\mathcal{K}^* - \mathcal{L}^*}{\mathcal{K}^*} = 0 \quad (95)$$

where n is the number of units in the system.

Proof. Recovering a feasible solution for the LR model requires adjusting the status of at most $2T$ units [31]-[32]. Therefore, the maximum adjustment cost is to make $2T$ units with the highest operation cost switch from off-status to on-status and keep the on-status for T period. Therefore, v_2^{LR} satisfy

$$v_2^{\mathrm{LR}} \le \max\{C_g^{\mathrm{start}}\} \cdot 2T + \max\{f_g(P_g^{\min}, 1)\} \cdot 2T^2, \forall g \quad (96)$$

Proposition 1 proves that $v_1 \le v_1^{\mathrm{LR}}$. Therefore, we have

$$v_1 \le v_1^{\mathrm{LR}} \le v_2^{\mathrm{LR}} \quad (97)$$

Taking (96) into (97) gives

$$v_1 \le \max\{C_g^{\mathrm{start}}\} \cdot 2T + \max\{f_g(P_g^{\min}, 1)\} \cdot 2T^2, \forall g \quad (98)$$

Then, for a system containing n units for the load D, the average output of the units $\overline{P}$ can be expressed as

$$\overline{P} = D / n \quad (99)$$

We approximate the generation cost function as a linear function $h_g(P) = a_g + b_g P$ (a_g,b_g represent the cost coefficient of unit g), and denote by $h^{\min}(P)$ the cost function with the lowest marginal cost $b^{\min}$. The optimal value $\mathcal{K}^*$ is greater than the generation cost that all loads are satisfied by the units with the lowest marginal cost $b^{\min}$. It follows that

$$\mathcal{K}^* \ge n \cdot h^{\min}(\overline{P}) \quad (100)$$

and then,

$$\frac{v_1}{\mathcal{K}^*} \le \frac{\max\{C_g^{\mathrm{start}}\} \cdot 2T + \max\{f_g(P_g^{\min}, 1)\} \cdot 2T^2}{n \cdot h^{\min}(\overline{P})} \quad (101)$$

Given any positive number ε (ε>0), take $N = \left[\left(\max\{C_g^{start}\}\cdot 2T + \max\{f_g(P_g^{\min},1)\}\cdot 2T^2\right)/\varepsilon h^{\min}(\bar{P})\right]$, we have $\left(\mathcal{K}^* - \mathcal{L}^*\right)/\mathcal{K}^* \le \varepsilon$ when $n > N$.

Therefore, $\lim_{n\to\infty} \frac{v_1}{\mathcal{K}^*} = \frac{\mathcal{K}^* - \mathcal{L}^*}{\mathcal{K}^*} = 0$. **(Q.E.D.)**

Proposition 1 proves that the proposed LP model can provide an initial solution that is at least as good as that of the LR model. In general, a better initial solution can deduce a better feasible solution under the same method of recovering a feasible solution. Therefore, we will generally have $v_2 \le v_2^{LR}$, which indicates that the feasible solution construction error of the LP model is always smaller than that of the LR model. **Proposition 2** points out that the error of the LP model decreases with the increase of the number of units, especially when the number of units tends to infinity. Therefore, the LP model of the multi-UC is suitable for large-scale SCUC models. The numerical experiments in the next section will verify the aforementioned phenomena.

IV. Case Study

In this section, we first verify the proposed strategy of embedding two types of convex hulls in the multi-UC using IEEE test systems. Then, we investigate the performance of the optimal solution of the proposed LP model of the single-UC with hydro units. Finally, comparable studies are done by applying the proposed LP model, the LR model, and the MILP model on provincial power systems to show the computational performance. Numerical results are conducted on a computer with 128 GB RAM and an Intel(R) Xeon(R) CPU E5-2650 processor.

A. The strategy of embedding two types of convex hulls in the multi-UC

We first present the basic information of several IEEE test systems. TABLE I and Fig.3 show the numbers of the buses, the transmission lines, the original thermal units, the thermal units reformulated by $\mathcal{G}$-convex hulls, and the thermal units reformulated by $\mathcal{E}$-convex hulls. It can be found that most units use the $\mathcal{E}$-convex hull to reduce the scale of the model. This is because there are many units with small capacity and high ramping rate, while a small number of units with large capacity and minimum-up/-down time.

TABLE I. The information of IEEE standard systems

Number of buses	Number of lines	Number of original units	Number of $\mathcal{G}$	Number of $\mathcal{E}$
118	186	54	12	42
300	411	69	11	58
1354	1991	260	32	228
2383	2896	327	56	271

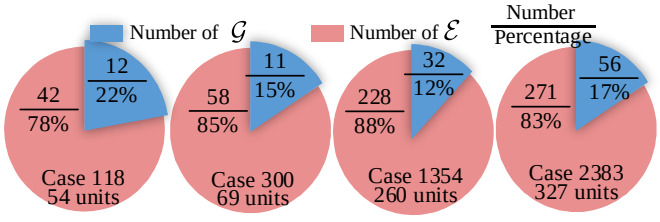

Fig.3 Percentage and number of units with two convex hulls

We next compare the computational performance of four models. Specifically, the original MILP model, the model using $\mathcal{G}$-convex hull only (denoted as "$\mathcal{G}$ only"), the model using $\mathcal{E}$-convex hull only (denoted as "$\mathcal{E}$ only"), and the model using embedding strategy (denoted as "ES") are compared in terms of computational time (in seconds), as shown in TABLE II, where the original MILP model is 1-2 orders of magnitude slower than the "$\mathcal{G}$ only", "$\mathcal{E}$ only", and "ES" models. Moreover, the computational time of the "$\mathcal{G}$ only" model is the slowest while that of the "ES" model is the fastest. Fig.4 visually shows the acceleration ratio of "$\mathcal{E}$ only" and "ES", with the "$\mathcal{G}$ only" model as the benchmark. The "$\mathcal{G}$ only" model is about 20% slower than the "$\mathcal{E}$ only" model because fewer units use the $\mathcal{G}$-convex hull, accounting for only about one-sixth of all units. Furthermore, the computational time of the "ES" model is 50%-60% of the "$\mathcal{G}$ only" model and 70%-85% of the "$\mathcal{E}$ only" model. The computational efficiency improvement of the "ES" model relies on (74) to filter out extreme units (e.g., the unit with T^{on}=1 or R^1<<P^{max}-P^{min}). These extreme units have a good performance under one convex hull but a poor performance under the other. Therefore, the effect of the proposed embedding strategy is reducing the model size and improving the computational performance by avoiding choosing the convex hull for the extreme units with poor computational performance.

In addition, the relative errors $v_2/\overline{\mathcal{L}^*}$ (v_2 is defined in (85)) of the IEEE 118-bus system, the IEEE 300-bus system, the IEEE1354-bus system, and the IEEE 2383-bus system are 1.97%, 0.92%, 0.63%, and 0.58%, respectively. The relative errors of a specific system are the same under the "$\mathcal{G}$ only" model, "$\mathcal{E}$ only" model, and "ES" model. This is because the $\mathcal{G}$ convex hull and the $\mathcal{E}$ convex hull are equivalent under any piecewise linear objective. (i.e. the $\mathcal{E}$-convex hull and the $\mathcal{G}$-convex hull have the same tightness). It suggested that the "ES" model that carefully chooses the correct convex hull formulations does perform better than any other formulations, and the strategy of embedding two types of convex hulls in a multi-UC can significantly improve computational efficiency.

TABLE II. The computational performance of four models

Buses	MILP	$\mathcal{G}$ only		$\mathcal{E}$ only		ES	
	Time(s)	Time(s)	Error	Time(s)	Error	Time(s)	Error
118	15	2.77	1.97%	2.36	1.97%	1.52	1.97%
300	127	3.86	0.92%	3.27	0.92%	2.33	0.92%
1354	830	65	0.63%	48	0.63%	38	0.63%
2383	4200	128	0.58%	96	0.58%	69	0.58%

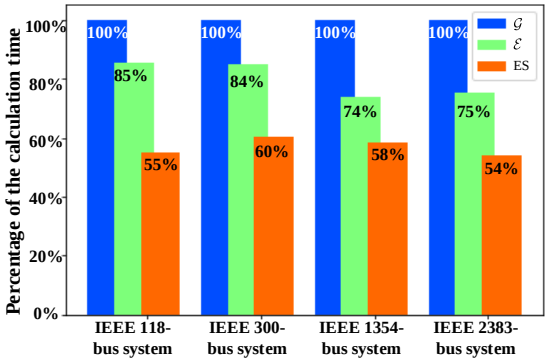

Fig.4 Percentage of the computational time

B. Test of the LP model of hydro single-UC

In this part, we investigate the relative error caused by the proposed LP model for hydro single-UC. We use the modified IEEE 300-bus system where 2, 4, 6, and 8 thermal units are replaced by the hydro units, respectively. Then, comparing the optimal values of the LP model and the MILP model, we can calculate the relative error $v_2/\mathcal{L}^*$ (v_2 is defined in (85)). The optimal values and the relative errors are shown in Fig.5. Because the hydro units work without fuel consumption, the optimal value is reduced from \$9.02M to \$8.31M with the increase in the number of hydropower units. Besides, the optimal value of the LP model becomes worse, and the relative error $v_2/\mathcal{L}^*$ increases from 1.73% to 1.82%. This is because the LP model of the single-UC with the hydro unit will introduce system constraints. For example, a normal hydro unit introduces T constraints, and a pump storage station introduces $3T$ constraints. Thus, more hydropower units will introduce more system constraints and the error will become larger.

According to the model (67)-(70), there are $(|L|+2+3|H|)T$ system constraints, where $3|H|T$ system constraints are introduced by hydro units. Note that $3|H|$ is far less than $(|L|+2)$, so the relaxation error resulting from the proposed LP model of hydro units is very small. When the number of hydro units in the IEEE 300-bus system increases from 0 to 2, 4, 6, and 8, the relative error of the LP model increases from 1.73% to 1.74%, 1.76%, 1.79%, and 1.82%. Nevertheless, as the number of hydro units is increased from 0 to 8 (10% of the number of units), the error is increased by only 0.09%. It suggested that the relative error caused by the proposed LP model for hydro single-UC is small, which meets the engineering need.

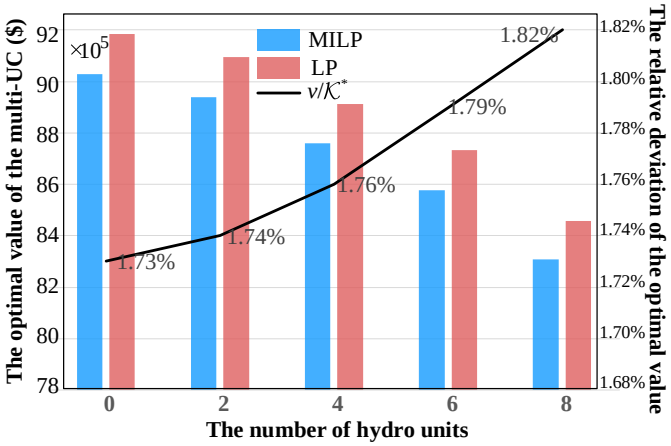

Fig.5 Optimal values and the relative error of multi-UC

C. Large-scale provincial power systems in China

We further apply the proposed LP model of the multi-UC to large-scale provincial power systems in China including Shaanxi, Ningxia, Qinghai, Gansu, Guangdong, and Guangxi, as well as regional power systems including Northwest China and Beijing-Tianjin-Tanggu (BTT), to demonstrate the effectiveness and efficiency of the proposed method. The dispatching periods are 24h(one day), 168h(one week), and 720h(one month). The multi-UC with long time horizons is a meaningful and practical problem that power dispatching and operation departments face. This is because the monthly UC has the properties of a "better-dispatching economy", "more detailed models for minimum-up/-down time limits and maintenance plans", and "better matching of contract evaluation methods". The information of the provincial systems is shown in TABLE III. Taking the MILP model as a benchmark which is solved by GUROBI commercial solver. The relative error and computational time of the MILP model, the LP model, and the LR model are compared.

TABLE III The information of provincial systems

Cases	Buses	Units [thermal/hydro]	Lines
Guangxi(220kV)	297	74 [59/15]	413
Ningxia	600	112 [110/2]	847
BTT	1600	154 [144/10]	2005
Guangdong	2350	181 [167/14]	2356
Qinghai	987	202 [164/38]	1203
Shaanxi	933	204 [200/4]	1256
Gansu	1387	311 [280/31]	1756
Xinjiang	3041	404 [378/26]	3457
Northwest China	6918	1233 [1136/97]	8519

We compare the above three models under three sets of optimality gaps (lengths of the operational horizon): 0.1% (T=24h), 0.5% (T=168h), and 1% (T=720h), respectively. The errors of the LR model v_2^{LR} and the LP model v_2 are listed in TABLE IV. In terms of the optimal value, the MILP model (benchmark) is the best while the LR model is the worst. The LP model performs between the MILP and LR models. Comparing the LP model with the LR model, we can have the following two conclusions. (i) As the power system size increases, the relative error of both two models become smaller. For example, when T=24h and the number of units rises from 74 in Guangxi to 1233 in Northwest China, the relative error $v_2^{\mathrm{LR}}/Z^{\mathrm{LR}*}$ (duality gaps) of the LR model decrease from 2.67% to 0.56%, and the relative error $v_2/\mathcal{L}^*$ of the LP model decreases from 2.53% to 0.52%. This verifies the conclusion that the relative error of the LP model mainly depends on the unit numbers n. (ii) As the number of scheduling periods (i.e., T) increases, the optimal values and convergence performance of the LR model become worse, while those of the LP model are hardly affected by T. For example, when T increases from 24h to 720h for Qinghai, the relative error of the LR model increase from 1.33% to 3.14%, but that of the LP model varies around 1%. It is suggested that the relative error of the proposed LP model for hydrothermal scheduling is small, meeting the engineering need.

In terms of computational time, the LP model is the fastest, while the MILP model is the slowest. The results show that the computational time of the MILP model is 1~2 orders of magnitude longer than that of the LR model and LP model, and the computational time of the LR model is 1~4 times longer than that of the LP model. Moreover, it can be found that the computational time of the two models increases nearly linearly with the increase of T. This is because the time complexity of both the $\mathcal{E}$-convex hull and the subproblems of the LR model is $O(T)$. However, the computational time of the LR model grows faster than that of the LP model. For example, when T increases from 24h, 168h to 720h for Shaanxi, the computational time of the LR model is 2.4, 2.7, and 2.9 times slower than that of the LP model. Most importantly, MILP may fail to obtain the optimal solution within the given time for some large-scale systems because the salability of MILP will

be challenged by the number of binary variables. The LR model may not be converged for long-term scheduling problems. The reason is that the LR model is solved iteratively, and the number of iterations increases with the increase of *T*. In contrast, the LP model can be easily solved by advanced and mature commercial solvers, without considering convergence issues. Therefore, the proposed LP model overperforms the LR model in both optimal solution and computational time.

TABLE IV. The computational time (seconds) and optimal solution error (%) of the three algorithms

	24h			168h			720h		
	MILP	LR	LP model	MILP	LR	LP model	MILP	LR	LP model
Guangxi(220kV)	43	13(2.67)	5.2(2.53)	817	78(4.25)	35.8(2.77)	1894	//	94.6(2.91)
Ningxia	158	22(2.48)	12(2.45)	1648	185(3.74)	84(2.19)	9904	//	336(2.68)
BTT	264	44(2.26)	18(2.08)	2762	369(2.94)	140(2.05)	16587	//	560(2.23)
Guangdong	186	31(1.68)	16(1.66)	1911	256(2.38)	113(1.68)	11476	1064(4.57)	459(1.73)
Qinghai	311	40(1.33)	18(0.96)	3278	340(1.66)	126(1.02)	#	1431(3.14)	504(1.16)
Shaanxi	332	43(1.57)	18(1.34)	3536	355(2.23)	133(1.54)	#	1494(3.82)	504(1.68)
Gansu	900	65(1.26)	39(1.12)	10708	520(1.78)	273(1.33)	#	2241(2.43)	1092(1.41)
Xinjiang	1580	82(0.91)	42(0.88)	#	749(0.95)	294(0.93)	#	2969(1.26)	1176(0.83)
Northwest China	9230	266(0.56)	128(0.52)	#	2758(0.63)	896(0.58)	#	14435(0.87)	3612(0.61)

Note: "#" indicates that the optimal solution cannot be obtained in 12 hours; "//" indicates that the duality gap cannot converge within 5%

V. Conclusion

This paper proposes an LP model for solving large-scale hydro-thermal unit commitment, where the LP model of the hydro single-UC is derived and the strategy of embedding two types of convex hulls in the multi-UC are proposed. Simulation results on several large-scale provincial systems show that the LP model of the single-UC with hydro units has a small effect on the optimal solution. Besides, the proposed embedding strategy can significantly improve the computational performance, compared with embedding either one type of convex hull. Moreover, it is shown that the proposed method is faster than both Lagrangian relaxation and commercial solvers. Moreover, the error gap of the proposed method is less than the Lagrangian relaxation method and the gap decreases with the increasing system scales. Finally, it is suggested that the proposed method can be well applied to large-scale long-term unit commitment problems.

References

[1] S. M. Hosseini, R. Carli and M. Dotoli, "Robust Optimal Energy Management of a Residential Microgrid Under Uncertainties on Demand and Renewable Power Generation," *IEEE Trans. Autom. Sci. Eng.*, vol. 18, no. 2, pp. 618-637, April 2021.

[2] F. Teng and G. Strbac, "Full Stochastic Scheduling for Low-Carbon Electricity Systems," *IEEE Trans. Autom. Sci. Eng.*, vol. 14, no. 2, pp. 461-470, April 2017.

[3] T. Ding, Z. Wu, J. Lv and et al, "Robust Co-Optimization to Energy and Ancillary Service Joint Dispatch Considering Wind Power Uncertainties in Real-Time Electricity Markets, *IEEE Trans. Sustain Energy*," vol. 7, no. 4, pp. 1547-1557, 2016.

[4] T. Ding, Z. Wang and et al , "A Sequential Black-Start Restoration Model for Resilient Active Distribution Networks," *IEEE Trans. Power Syst.*, vol. 37, no. 4, pp. 3133-3136, July 2022.

[5] Y. Fu and M. Shahidehpour, "Fast SCUC for Large-Scale Power Systems," *IEEE Trans. Power Syst.*, vol.22, no.4, pp.2144-2151, Nov. 2007.

[6] S. Virmani, E. C. Adrian, K. Imhof and S. Mukherjee, "Implementation of a Lagrangian relaxation based unit commitment problem," *IEEE Trans. Power Syst.*, vol. 4, no. 4, pp. 1373-1380, Nov. 1989.

[7] Q. Zhai, X. Guan, and J. Chen, "Unit commitment with identical units successive subproblem solving method based on Lagrangian relaxation," *IEEE Trans. Power Syst.*, vol. 17, no. 4, pp. 1250-1257, 2002.

[8] Y. Fu, M. Shahidehpour and Z. Li, "Long-term security-constrained unit commitment: hybrid Dantzig-Wolfe decomposition and subgradient approach," *IEEE Trans. Power Syst.*, vol. 20, no. 4, pp. 2093-2106, 2005.

[9] B. Sun, P. B. Luh, Q. Jia and B. Yan, "Event-Based Optimization within the Lagrangian Relaxation Framework for Energy Savings in HVAC Systems," *IEEE Trans. Autom. Sci. Eng.*, vol. 12, no. 4, pp. 1396-1406, Oct. 2015.

[10] L. L. Garver, "Power generation scheduling by integer programming-development and theory," *Trans. Amer. Inst. Elect. Eng. Part III: Power App. Syst.*, vol. 81, no. 3, pp. 730-734, Apr. 1962.

[11] F. Safdarian, A. Mohammadi and A. Kargarian, "Temporal Decomposition for Security-Constrained Unit Commitment," *IEEE Trans. Power Syst.*, vol. 35, no. 3, pp. 1834-1845, May 2020.

[12] A. Street, A. Moreira and J. M. Arroyo, "Energy and reserve scheduling under a joint generation and transmission security criterion: An adjustable robust optimization approach," *IEEE Trans. Power Syst.*, vol. 29, no. 1, pp. 3-14, Jan. 2014.

[13] J. Aghaei, M. Karami, K. M. Muttaqi, H. A. Shayanfar and A. Ahmadi, "MIP-Based Stochastic Security-Constrained Daily Hydrothermal Generation Scheduling," *IEEE Syst. Jour.*, vol. 9, no. 2, pp. 615-628, 2015.

[14] X. Li, T. Li, J. Wei, G. Wang, "Hydro Unit Commitment via Mixed Integer Linear Programming: A Case Study of the Three Gorges Project, China," *IEEE Trans. Power Syst.*, vol. 29, no. 3, pp. 1232-1241, May 2014.

[15] Y. Chen, F. Liu, B. Liu, W. Wei and S. Mei, "An Efficient MILP Approximation for the Hydro-Thermal Unit Commitment," *IEEE Trans. Power Syst.*, vol. 31, no. 4, pp. 3318-3319, July 2016.

[16] Y. Fu, Z. Li and L. Wu, "Modeling and solution of the large-scale security-constrained unit commitment", *IEEE Trans. Power Syst.*, vol. 28, no. 4, pp. 3524-3533, Nov. 2013.

[17] https://www.gurobi.com/

[18] https://www.ibm.com/analytics/cplex-optimizer

[19] X. Li, Q. Zhai, J. Zhou and X. Guan, "A Variable Reduction Method for Large-Scale Unit Commitment," *IEEE Trans. Power Syst.*, vol. 35, no. 1, pp. 261-272, Jan. 2020.

[20] T. Ding et al., "Fast identifying redundant security constraints in SCUC in the presence of uncertainties," *IET Gener. Trans. Dis.*, vol. 14, no. 13, pp. 2441-2449, 2020.

[21] C. Zhao and Y. Guan, "Unified Stochastic and Robust Unit Commitment," *IEEE Trans. Power Syst.*, vol. 28, no. 3, pp. 3353-3361, 2013.

[22] R. Lu, T. Ding, B. Qin, J. Ma, X. Fang and Z. Dong, "Multi-stage stochastic programming to joint economic dispatch for energy and reserve with uncertain renewable energy," *IEEE Trans. Sustain. Energy*, vol. 11, no. 3, pp. 1140 - 1151, 2019.

[23] Y. Guan and J. Wang, "Uncertainty Sets for Robust Unit Commitment," *IEEE Trans. Power Syst.*, vol. 29, no. 3, pp. 1439-1440, 2014.

[24] T. Ding et al., "Multi-Stage Distributionally Robust Stochastic Dual Dynamic Programming to Multi-Period Economic Dispatch With Virtual Energy Storage," *IEEE Trans. Sustain. Energy*, vol. 13, no. 1, pp. 146-158, Jan. 2022.

[25] B. Yan, and et al, "A systematic formulation tightening approach for unit commitment problems," *IEEE Trans. Power Syst.*, vol.35, no.1, pp.782-794, 2019.

[26] Y. Yu, Y. Guan and Y. Chen, "An Extended Integral Unit Commitment Formulation and an Iterative Algorithm for Convex Hull Pricing," *IEEE Trans. Power Syst.*, vol. 35, no. 6, pp. 4335-4346, Nov. 2020.

[27] S. Chen, Z. Wei, G. Sun, W. Wei and D. Wang, "Convex Hull Based Robust Security Region for Electricity-Gas Integrated Energy Systems," *IEEE Trans. Power Syst.*, vol. 34, no. 3, pp. 1740-1748, May 2019.
[28] J. Li and Z. Zhang, "Quick Algorithm for Unit Commitment Based on Relaxation and Neighborhood Search," *2018 14th International Conference on Natural Computation, Fuzzy Systems and Knowledge Discovery* (ICNC-FSKD), 2018, pp. 336-343
[29] B. Yan et al., "A Systematic Formulation Tightening Approach for Unit Commitment Problems," *IEEE Trans. Power Syst.*, vol. 35, no. 1, pp. 782-794, Jan. 2020.
[30] Y. Guan, K. Pan, and K. Zhou, "Polynomial Time Algorithms and Extended Formulations for Unit Commitment Problems," *IISE Trans.*, vol.50, no.8, pp.735, 2018.
[31] D. Bertsekas, G. Lauer, N. Sandell and T. Posbergh, "Optimal short-term scheduling of large-scale power systems," *IEEE Trans. Automat. Contr.*, vol. 28, no. 1, pp. 1-11, Jan. 1983.
[32] Dimitri Bertsekas and Nils Sandell. Estimates of the duality gap for large-scale separable nonconvex optimization problems. *1982 21st IEEE Conference on Decision and Control*, pages 782-785, 1982.
[33] X. Guan, S. Guo, and Q. Zhai, "The conditions for obtaining feasible solutions to security-constrained unit commitment problems," *IEEE Trans. Power Syst.*, vol. 20, no. 4, pp. 1746-1756, 2005.
[34] J.J.Shaw, "A direct method for security-Constrainted Unit," *IEEE Trans. Power Syst.*, vol.10, no.3, pp.1329-1342, 1995.
[35] D. Apostolopoulou and M. McCulloch, "Optimal Short-Term Operation of a Cascaded Hydro-Solar Hybrid System: A Case Study in Kenya," *IEEE Trans. Sustain. Energy*, vol. 10, no. 4, pp. 1878-1889, Oct. 2019.
[36] F. A. Al-Khayyal and J. E. Falk, "Jointly constrained biconvex programming," *Math. Oper. Res.*, vol. 8, no. 2, pp. 273–286,1983.
[37] P. Andrianesis, D. J. Bertsimas, M. Caramanis and W. Hogan, "Computation of Convex Hull Prices in Electricity Markets with Non-Convexities using Dantzig-Wolfe Decomposition," *IEEE Trans. Power Syst.*, vol. 37, no. 4, pp. 2578-2589, July 2022.
[38] A. Wood and B. Wollenberg, "Unit Commitment," in *Power generation, operation, and control*, 2nd ed. Canada: John Wiley & Sons Inc, 1996, ch.5, sec.2, pp.139-141.
[39] T. Ding, Q. Yang, X. Liu, et al, "Duality-free decomposition based data-driven stochastic security-constrained unit commitment", *IEEE Trans. on Sustain. Energy*, vol. 10, no. 1, pp. 82-93, 2019.